Biophysical Chemistry 21 (1985) 201–209
Elsevier

BPC 00907c

APPENDIX B TO ARTICLE BPC 00907a

VARIATION OF THE SHUTTLING CONSTANTS FOR RECYCLING RECEPTORS

Paul W. CHUN

Note: The references cited herein are listed on pages 195 and 196 of article BPC 00907a

The macromolecular species distribution in a receptor-mediated endocytotic pathway, determined by computer simulation based on kinetic data reported in the literature [44,46,47,55], suggests that the shuttling constant for the recycling of transferrin or insulin receptors back to the surface depends not only on the type of cell used in the experiment but also upon the reversibility of ligand binding to the cell surface receptor.

The magnitude of the shuttling constants will vary with the experimental conditions, but when the value is large, the internalized receptor is quickly shuttled back to the cell surface. When this value is small, however, the time required to traverse the entire endocytotic pathway is much longer.

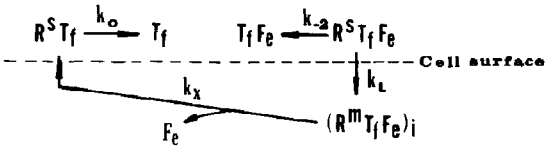

Fig. 11. Proposed kinetic pathway for single-cycle receptor-mediated endocytosis of transferrin in which apotransferrin is liberated into the medium in HepG2 cells. $T_f F_e$ represents ferrotransferrin; R^S, unoccupied surface receptor; $R^S T_f F_e$, surface ferrotransferrin-receptor complex. $R^m T_f F_e$ is the intracellular ferrotransferrin-receptor complex. $R^S T_f$ is the surface apotransferrin-receptor complex; T_f, apotransferrin. k_0 represents the rate constant for dissociation of apotransferrin from cell surface receptors as all functional receptors behave identically, k_{-2}, rate constant for dissociation of ferrotransferrin from cell surface receptors. k_L, rate constant for internalization of surface ferrotransferrin-receptor complex. k_X, overall shuttling rate constant for dissociation of iron and movement of the apotransferrin receptor complex to the cell surface.

B1. Case I: Single-cycle receptor-mediated endocytosis of transferrin in HepG2 cells [44]

Transferrin is a serum glycoprotein that transports iron from sites of absorption and storage to tissue cells. After endocytosis, the transferrin is not degraded, but is exocytosed intact into the medium [43,44]. Current structural information indicates that transferrin receptors in human leukemia cells are disulfide-linked dimers, having a molecular weight of 180 000 [45]. Growing hepatoma G2 cells contain approx. 50 000 functional surface binding sites for transferrin and 100 000 intracellular sites [44].

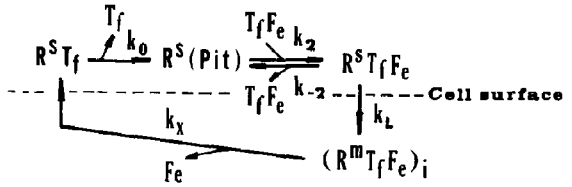

Fig. 12. Proposed kinetic pathway for single-cycle receptor-mediated endocytosis of transferrin in the steady state in HepG2 cells. Transferrin ($T_f F_e$) binds to a specific cell surface receptor (R^S), and the receptor-transferrin complex, ($R^S T_f F_e$), is internalized in clathrin-coated pits and vesicles, $(R^m T_f F_e)_i$, followed by dissociation of F_e from the receptor in an endosome vesicle, and $R^S T_f$ is then transported into the cell surface.

Table 2

Kinetic parameters for receptor-mediated endocytosis: transferrin and insulin

Parameters	Transferrin (hepatoma cell, hepG2)	Insulin (3T3 L-1 adipocytes/10^6 cells)	
(A) Receptor-synthesis	$[R^s]$ or $[R^m]$	$[R^s]$ or $[R^m]$ [56]	$[R^s]$ or $[R^m]$ [56]
$k_1[A]$ (pmol/h)	–	0.0075	0.0075
(B) Ligand binding	$[k_2T_fF_e]$ [43]	$[k_2I]$ (h^{-1})	$[k_2I]$ (h^{-1}) [47,48]
k_2X (min^{-1} or h^{-1})	0.23	0.70	0.30
$t_{1/2}$ (min)	3.0 min	0.99 h	2.31 h
t_{mean}	4.35	1.43	3.33
(C) Dissociation of ligand from bound receptor $[I], [L] = X$	$[R^sT_fF_e] \rightarrow [T_fF_e]$ [43]	$[R^sI] \rightarrow [R^s]$	$[R^sI] \rightarrow [R^s]$ [47,48]
k_{-2} (min^{-1} or h^{-1})	0.09	–	0.125
$t_{1/2}$	7.7 min	–	5.54 h
t_{mean}	11.1	–	8.00
(D) Internalization of surface receptor	$[R^mT_fF_e]_i$ [43]	$[R^sI] \rightarrow [R^mI]$	$[R^sI] \rightarrow [R^mI]$ [47,48]
k_L (min^{-1} or h^{-1})	0.2	–	0.5
$t_{1/2}$	3.5 min	–	1.35 h
t_{mean}	5.0	–	2.0
(E) Movement of internalized receptors	$[R^m]$	$[R^mI] \rightarrow [R^m]$	$[R^mI] \rightarrow [R^m]$ [47,48]
k_{-3} (min^{-1} or h^{-1})	–	–	0.05
$t_{1/2}$	–	–	13.9 h
t_{mean}	–	–	20.0
(F) Appearance of internalized receptor at the cell surface	$[R^sT_f]$ [43]	$[R^m] \rightleftarrows [R^s]$	$[R^m] \rightleftarrows [R^s]$ [47,48]
k_{-m} or k_X (min^{-1} or h^{-1}) (k_m)	0.14	–	0.5 (1.0)
$t_{1/2}$ ($t^m_{1/2}$)	4.95 min	–	1.4 (0.7) h
t_{mean} (t^m_{mean})	7.14	–	2.0 (1.0)
(G) Dissociation of ligand from recycled receptor-bound ligand complex	$[R^sT_f] \rightarrow [R^s]$ [43]	–	–
k_0 (min^{-1} or h^{-1})	2.6	–	–
$t_{1/2}$	0.27	–	–
t_{mean}	0.38	–	–
(H) Degradation of receptor-ligand complex	$[R^mT_fF_e]_i$ or $[R^mT_f]_i$	$[R^mI] \rightarrow D$ [56]	$[R^mI] \rightarrow D$ [47,48]
k_d (min^{-1} or h^{-1})	–	0.103 h^{-1}	0.053
$t_{1/2}$	–	6.73 h	13.1 h
t_{mean}	–	9.71	18.9
t_{mean}, time required for a receptor to traverse the entire endocytotic cycle (t_R)	$t_R = [k_2T_fF_e]^{-1} + [k_X]^{-1} + [k_0]^{-1} + [k_L]^{-1} = 16.5$ min	$t_R = [k_2I] + [k_L]^{-1} + [k_{-3}]^{-1} + [k_{-m}]^{-1} = 27.33$ h/10^6 cells, (down-regulated state)	

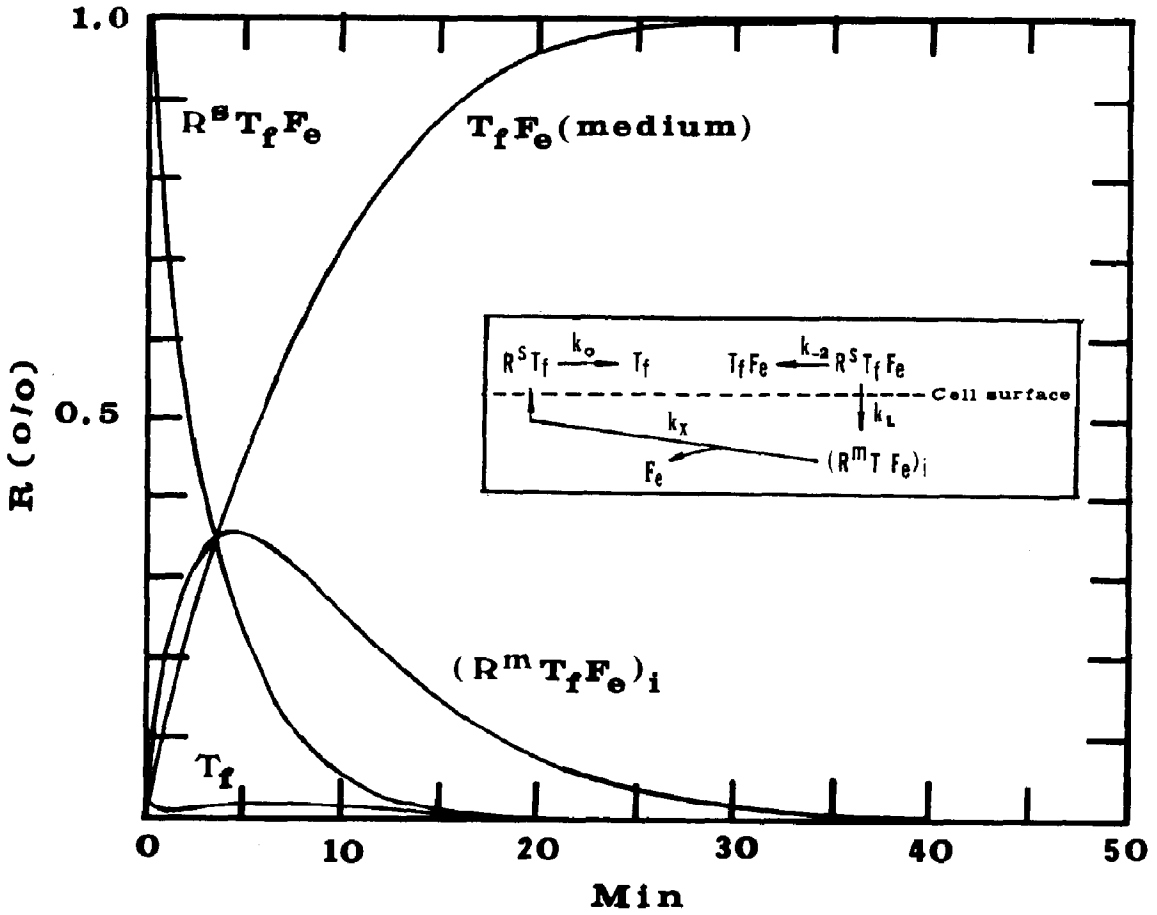

Fig. 13. Macromolecular endocytotic species distribution in single cycle receptor-mediated endocytosis of ^{125}I-transferrin in HepG2 cells. ^{125}I-transferrin bound to HepG2 cell receptors ($R^S T_f F_e$) at 4°C after washing was incubated at 37°C in the presence of 128 nM unlabeled transferrin containing 1.7 mM $CaCl_2$ as the experimental starting point. The cells were chilled and treated with pronase for 1 h at 4°C. The radioactivity in the pronase-resistant fraction, $[R^m T_f F_e]_i$; pronase-sensitive fraction, $[R^S T_f F_e]$; the medium, $[T_f F_e]$; and the appearance of apotransferrin-receptor complex, $[R^S T_f]$, were monitored. Experimental data were taken from ref. 44 $[R^S]_0$ at time zero, $[R^m T_f F_e] = 3\%$ (fraction), $[R^S T_f F_e] = 100\%$, $[R^S T_f] = 3\%$, $k_{-2} = 0.09$ min^{-1}, $k_0 = 2.6$ min, $k_L = 0.2$ min^{-1} and $k_X = 0.14$ min^{-1}. Kinetic plots shown were generated by the numerical simulation of four differential equations using the Runge-Kutta approximation. The global goodness of fit of the $\bar{R}^2$ value was 0.9993 and correlation coefficient of each data point of the fitted curve was 0.9996. $[R^S]_0 = 0$ at $t = 0$.

	T_f	$R^S T_f F_e$	$R^m T_f F_e$	$R^S T_f$
$\frac{d[T_f]_{medium}}{dt}$	0	k_{-2} (0.09)	0	k_0 (2.6)
$\frac{d[R^S - T_f F_e]}{dt}$	0	$-(k_{-2} + k_L)$ $-(0.29)$	0	0
$\frac{d[R^m - T_f F_e]_i}{dt}$	0	k_L $-(0.20)$	$-k_x$ $-(0.14)$	0
$\frac{d[R^S T_f]}{dt}$	0	0	k_x (0.14)	$-k_0$ $-(2.6)$

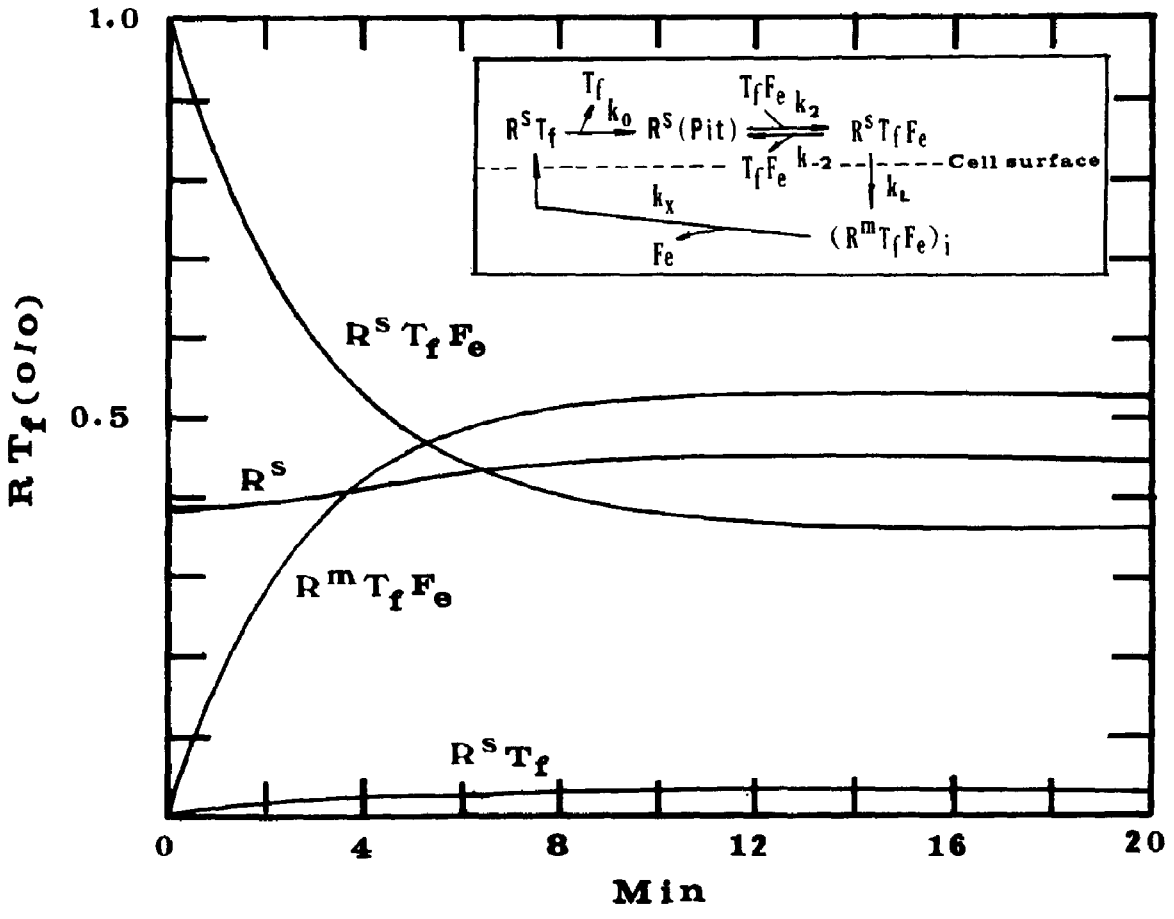

Fig. 14. Macromolecular species distribution of recycling transferrin receptors in HepG2 cells (a single-cycle receptor-mediated endocytosis in the steady state). Kinetic parameters used for simulation are identical to those in fig. 13 except that the percent fraction of $[R^s]$ was evaluated from initial steady-state conditions, where $k_2[T_fF_e][R^s]-(k_{-2}+k_L)[R^sT_fF_e]=0$. Then $[R^s]=39\%$, fraction of free cell surface receptor if $[R^sT_fF_e]=1.0$, $k_2[T_fF_e]=0.23\ min^{-1}$ and $(k_{-2}+k_L)=0.29\ min^{-1}$. Kinetic plots shown were generated by the numerical simulation of four differential equations using the Runge-Kutta method.

	T_f	R_s	$R^s-T_fF_e$	$R^m-T_fF_e$	R^s-T_f
$\frac{d[R^s]}{dt}$	0	$-k_2T_fF_e$	k_{-2}	0	k_0
		$-(0.23)$	(0.09)		(2.6)
$\frac{d[R^s-T_fF_e]}{dt}$	0	$k_2T_fF_e$	$-(k_{-2}+k_L)$	0	0
		(0.23)	$-(0.29)$		
$\frac{d[R^m-T_fF_e]_i}{dt}$	0	0	k_L	$-k_x$	0
			(0.2)	$-(0.14)$	
$\frac{d[R^s-T_f]}{dt}$	0	0	0	k_x	$-k_0$
				(0.14)	$-(2.6)$

The steady-state uptake of ligand is described by the kinetic models shown in figs. 11 and 12. In these models, there is no evidence that the ligand-receptor binding event promotes the entry and subsequent activity of a degradation (k_d) of the $[R^mT_fF_e]_i$ intracellular ferrotransferrin-receptor complex, and synthesis of cell surface receptor, $[R^s]$. The total receptor concentration may be expressed as $[R]_T = [R^s] + [R^sT_fF_e] + [R^sT_f] + [R^mT_fF_e]_i$ and there is no evidence of an intracellular pool of receptors not bound to transferrin.

The macromolecular species distribution of transferrin in a single-cycle endocytotic pathway in which apotransferrin (T_f) is liberated into the medium is shown in fig. 13, based on the four differential equations which follow. This kinetic plot is identical to that reported by Ciechanover et al. [44].

$$\frac{d[R^s]}{dt} = k_{-2}[R^s - T_fF_e] - k_2[T_fF_e][R^s] + k_0[R^s - T_f]$$

$$\frac{d[R^s - T_fF_e]}{dt} = k_2[T_fF_e][R^s] - (k_{-2} + k_L)[R^s - T_fF_e]$$

$$\frac{d[R^m - T_fF_e]_i}{dt} = k_L[R^s - T_fF_e] - k_X[R^m - T_fF_e]_i$$

$$\frac{d[R^sT_f]}{dt} = k_X[R^m - T_fF_e]_i - k_0[R^s - T_f],$$

where

$$\frac{d[T_f]_{medium}}{dt} = k_0[R^s - T_f] + k_{-2}[R^s - T_fF_e]$$

Fig. 4 shows the macromolecular species distribution of recycling transferrin receptors in a single-cycle, receptor-mediated endocytotic pathway in the steady state, based on the four differential equations shown above. At the initial steady-state condition, $d[R^sT_fF_e]/dt = 0$; no internalization takes place. Thus, the concentration of the surface receptor is 0.39 (wt%), i.e., $k_2[T_fF_e][R^s] - (k_{-2} + k_L)[R^s - T_fF_e] = 0$ where $[R^sT_fF_e] = 1.0$, $k_{-2} = 0.9$ min^{-1} and $(k_{-2} + k_L)$ was found to be 0.29 min^{-1}, as shown in table 2. In a single-cycle system such as this, the shuttling constant, k_X, was 0.14 min^{-1}, an indicator of rapid recycling, while the half-life time, $t_{1/2}$, was 5 min. The time required to traverse a single cycle was found to be 16.5 min, identical to the value reported previously by Ciechanover et al. [44]. The species distribution reached a steady state after 8 min and the concentration of surface receptor remained relatively constant throughout the cycle. At the steady state, the magnitudes of the two species ($[R^sT_fF_e]$, surface bound ferrotransferrin-receptor complex, and $[R^mT_fF_e]_i$, intracellular ferrotransferrin-receptor complex) maintained an equilibrium.

One problem with this particular kinetic model is that it fails to describe down-regulation by the degradation product, because no synthesis or down-regulation of cell surface receptor by ligand binding is involved.

B2. Case II: Regulation of insulin receptor metabolism in differentiating 3T3 L-1 adipocytes [46,47]

Human 3T3 L-1 adipocytes maintain a level of 25000 or 35000 site-specific insulin-binding sites per cell [48]. Treatment of 3T3 L-1 cells with insulin results in an initial suppression of insulin binding, followed by an increase to 170000 binding sites per cell in differentiating cells [48], forming what appears to be an intracellular pool of insulin receptor [49,50]. The insulin receptor undergoes an intracellular phosphorylation-dephosphorylation reaction [50–52] induced by the presence of insulin [50]. In addition to mediating such a reaction, insulin initiates regulation of various cellular processes by interacting with the specific cell surface receptor, a tetrameric glycoprotein consisting of two 125000 M_r subunits (α_2) and two 94000 M_r subunits (β_2) in a disulfide-linked complex [54]. The intracellular autophosphorylation reaction may be the primary signal by which a cell recognizes occupied receptors and eventually alters its receptor synthesis and degradation according to the magnitude and duration of this signal [50,54].

The up- and down-regulation kinetics of receptor synthesis and degradation, based on the numerical solution for six differential equations, are shown below (see fig. 15A–C).

$$\frac{d[R^m]}{dt} = k_1[A] + k_m[R^s] - k_{-m}[R^m] + k_{-3}[R^mI] - k_X[R^m]$$

$$\frac{d[R^s]}{dt} = k_{-m}[R^m] - k_m[R^s] + k_{-2}[R^sI] - k_2[R^s][I]$$

$$\frac{d[R^sI]}{dt} = k_2[R^s][I] - k_{-2}[R^sI]$$

$$\frac{d[R^*_sI]}{dt} = k_3[R^sI] - k_L[R^*_sI]$$

$$\frac{d[R^mI]}{dt} = k_L[R^*_sI] - (k_{-3} + k_d)[R^mI]$$

$$\frac{d[R^*_s]}{dt} = k_x[R^{m'}] - k_2[R^*_s][I]$$

The turnover rate of insulin receptors, k_d, was found to be 0.103 h^{-1}, the half-life, $t_{1/2}$, 6.73 h, and mean time 9.71 h [55,56]. Simulation of the six differential equations based on the kinetic models shown in fig. 16 by the Runge-Kutta method shows that the shuttling constant, k_{-3}, is 0.05 h^{-1}, while the half-life time, $t_{1/2}$, is 13.9 h, as seen in table 2. On the other hand, our kinetic simulation shown in fig. 17 resulted in a turnover rate of 0.053 h^{-1} and a half-life time of 13.1 h. The time required for the degradation of the receptor-insulin complex was found to be 19 h, twice as long as that reported by Reed and Lane [55].

Insulin receptor recycling time to traverse the entire endocytotic cycle was estimated to be 27.3 $h/10^6$ cells in differentiating 3T3 L-1 adipocytes as shown in fig. 16 and 18. Why does it take so long to traverse the entire cycle? Possibilities which would affect the shuttling constant are: (i) the reversibility of the ligand binding, which regulates translocation of receptors; (ii) the possible existence of an intracellular receptor pool; (iii) existence of a synchrony between receptor synthesis and degradation; and (iv) phosphorylation-dephosphorylation of receptor for signal modulation.

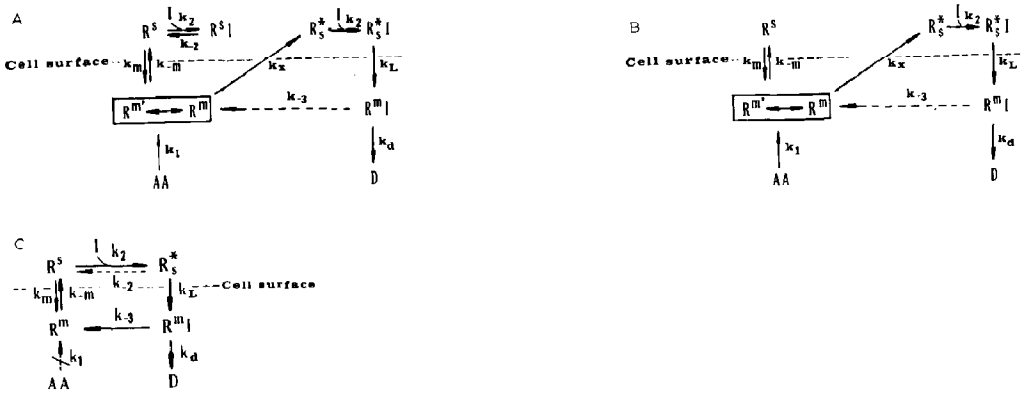

Fig. 15. (A) Proposed kinetic pathway for regulation of insulin receptor metabolism in differentiating 3T3-L1 adipocytes. R^s represents the cell surface receptors capable of binding insulin to form a receptor-insulin complex (R^sI) at the surface. Unlike the other receptor-mediated processes, the magnitude of reversibility of the ligand binding (k_{-2}) serves only to regulate recycling levels by translocation of receptors and in turn modulate the synthesis and degradation of receptor. The decrease in the level of cell surface receptor, as in one-way catalysis, in directly related to the ambient level of the insulin. The turnover and degradation of R^mI, internalized receptor-insulin complex, may thus depend on insulin concentration. R^*_sI, surface-bound insulin receptors, are also capable of controlling receptor levels, since a site-site interaction is involved. (B) Proposed kinetic pathway for translocation and regulation of insulin receptor metabolism in differentiating 3T3L-1 adipocytes (site-specific interaction). (C) Proposed kinetic pathway for degradation of insulin-receptor complex. Receptor synthesis is completely inhibited so that k_{-2} approaches zero.

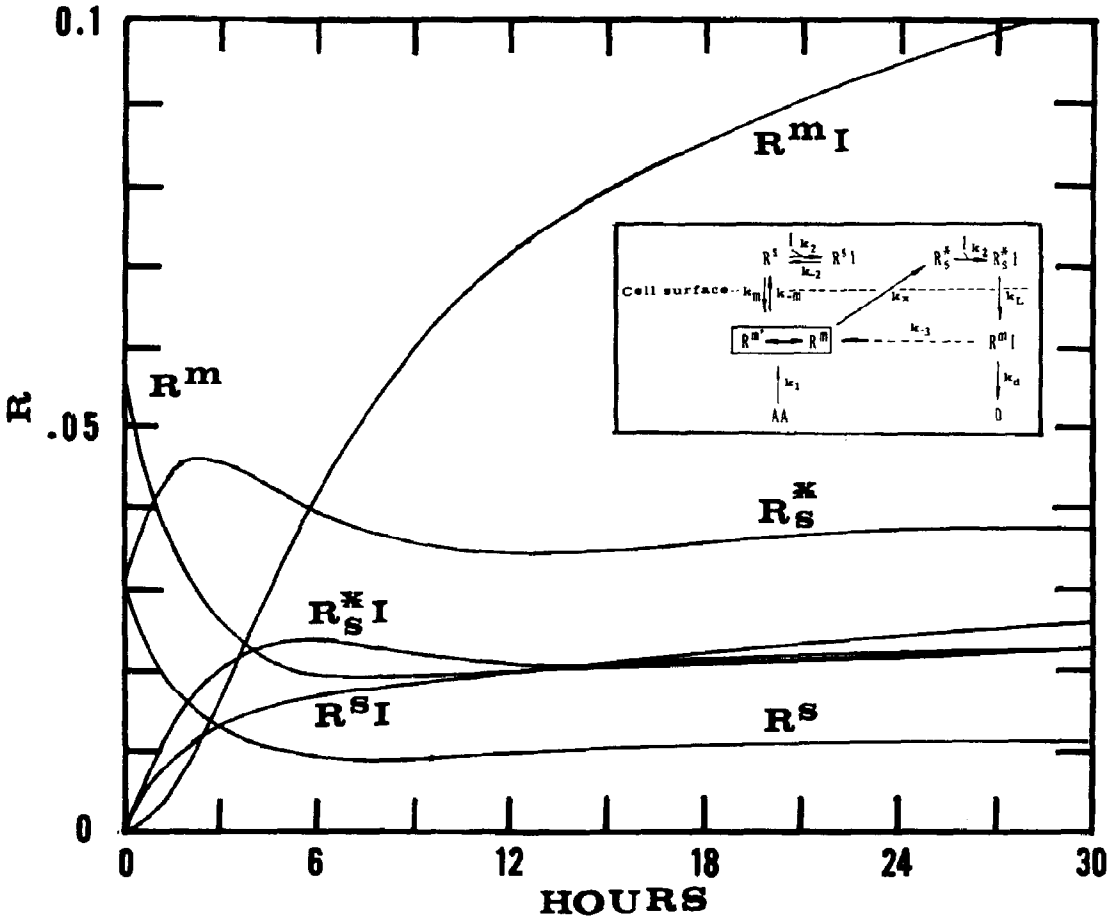

Fig. 16. Macromolecular distribution of receptor-insulin complexes in differentiating 3T3 L-1 adipocytes. Kinetic distribution plots shown were generated by numerical solution of six differential equations using the Runge-Kutta method. The kinetic parameters used for simulation are shown in table 2.

	k_1[A]	R^m	R_s^*	R_s^*I	R^mI	R^s	R^sI
$\frac{d[R^m]}{dt}$	k_1[A]	$-(k_x + k_{-m})$	0	0	$-k_{-3}$	k_m	0
	(0.0075)	−(1.0)			(0.05)	(1.0)	
$\frac{d[R_s^*]}{dt}$	0	k_x	$-k_2$[I]	0	0	0	0
		(0.5)	−(0.3)				
$\frac{d[R_s^*I]}{dt}$	0	0	k_2[I]	$-k_L$	0	0	0
			(0.3)	−(0.5)			
$\frac{d[R^mI]}{dt}$	0	0	0	k_L	$-(k_{-3} + k_d)$	0	0
				(0.5)	(0.103)		
$\frac{d[R^s]}{dt}$	0	k_{-m}	0	0	0	$-(k_m + k_2$[I])	k_{-2}
		(0.5)				−(1.30)	(0.125)
$\frac{d[R^sI]}{dt}$	0	0	0	0	0	k_2[I]	$-k_{-2}$
						(0.3)	−(0.125)

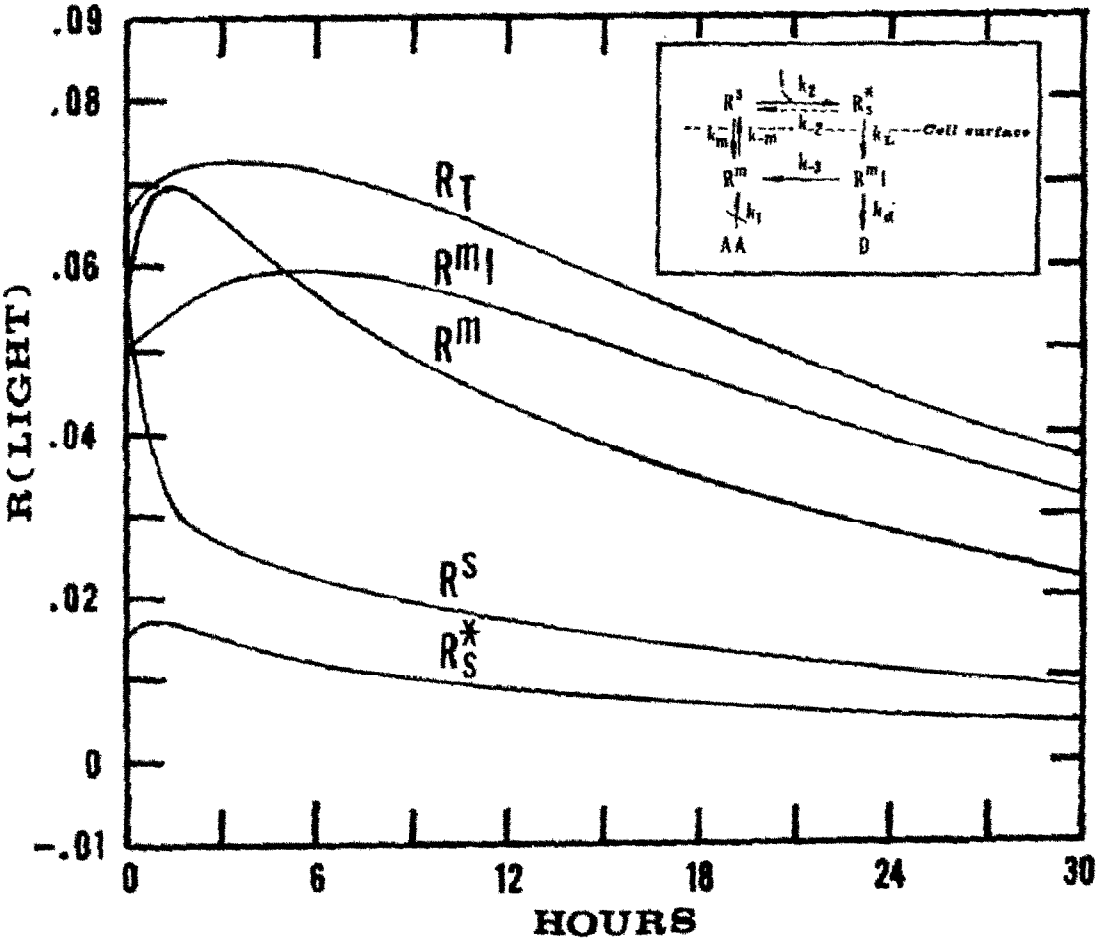

Fig. 17. Macromolecular distribution of receptor-insulin complexes and species degradation in differentiating 3T3 L-1 adipocytes at the steady state. Receptor synthesis is completely inhibited so that $k_1[A] = 0$ and k_{-2} approaches zero. Kinetic plots shown were generated by numerical solution of four differential equations using the Runge-Kutta method. $[R^m]_0 = 0.055$ pmol/10^6 cells, $[R^s]_0 = 0.06$ pmol/10^6 cells, $[R^*_sI] = 0.015$ pmol/10^6 cells, $[R^mI] = 0.05$ pmol/10^6 cells.

	$k_1[A]$	R^m	R^s	R^*_sI	R^mI
$\frac{d[R^m]}{dt}$	0	$-k_{-m}$	k_m	0	k_{-3}
		$-(0.5)$	(1.0)		(0.5)
$\frac{d[R^s]}{dt}$	0	k_{-m}	$-(k_m + k_2[I])$	0	0
		(0.5)	$-(1.3)$		
$\frac{d[R^*_sI]}{dt}$	0	0	$k_2[I]$	$-k_L$	0
			(0.3)	$-(0.5)$	
$\frac{d[R^mI]}{dt}$	0	0	0	k_L	$-(k_{-3} + k_d)$
				(0.5)	$-(0.103)$

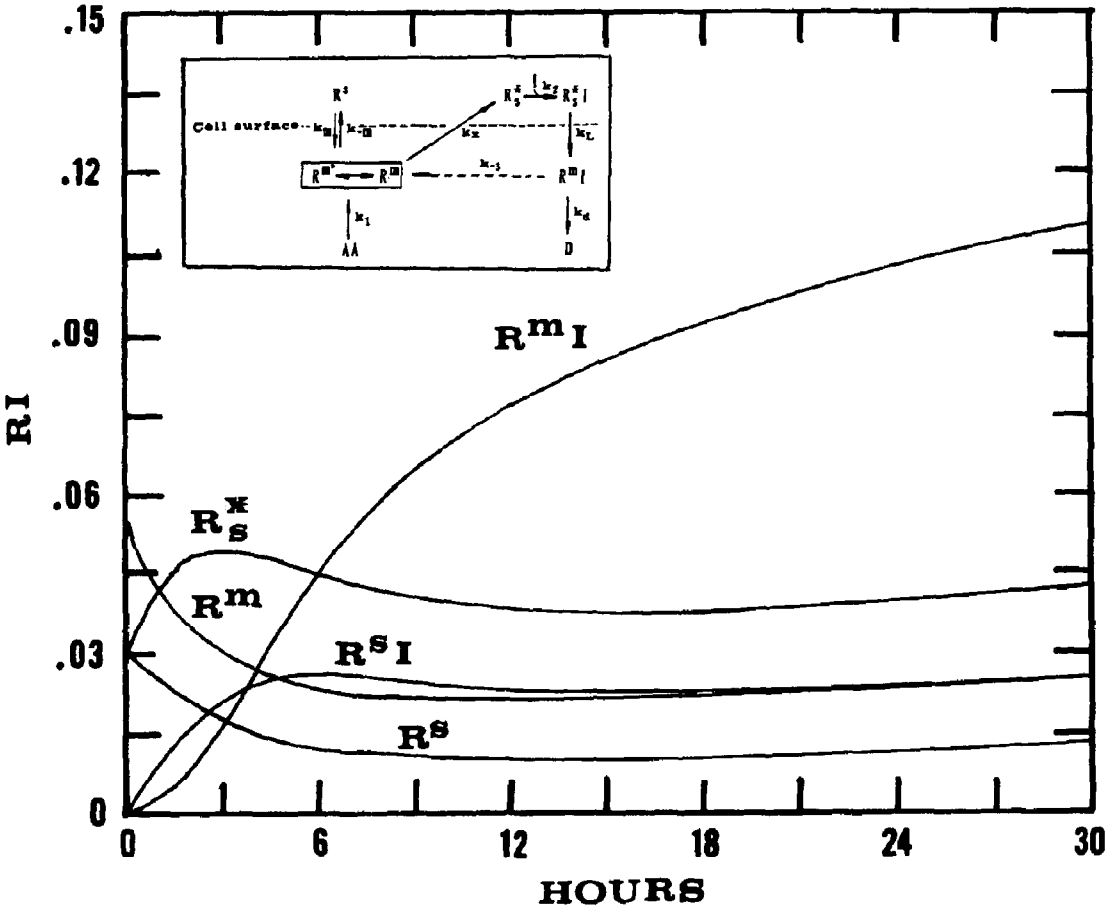

Fig. 18. Macromolecular distribution of receptor-insulin complexes and translocating receptor into intracellular compartments in differentiating 3T3 L-1 adipocytes. Kinetic distribution plots were generated by numerical solution of five differential equations using the Runge-Kutta method.

	$k_1[A]$	R^m	R^s	R_s^*	R_s^*I	R^mI
$\frac{d[R^m]}{dt}$	$k_1[A]$	$-(k_s + k_{-m})$	k_m	0	0	k_{-3}
	(0.0075)	$-(1)$	(1.0)			(0.05)
$\frac{d[R^s]}{dt}$	0	k_{-m}	$-k_m$	0	0	0
		(0.5)	$-(1.0)$			
$\frac{d[R_s^*]}{dt}$	0	k_x	0	$-k_2[I]$	0	0
		(0.5)		$-(0.3)$		
$\frac{d[R_s^*I]}{dt}$	0	0	0	$k_2[I]$	$-k_L$	0
				(0.3)	$-(0.5)$	
$\frac{d[R^mI]}{dt}$	0	0	0	0	k_L	$-(k_{-3} + k_d)$
					(0.5)	$-(0.103)$

$k_1[A] = 0.0075$ pmol/h, $[R^m]_0 = 0.055$ pmol/10^6 cells, $[R_s^*] = 0.03$ pmol/10^6 cells, $[R^s]_0 = 0.03$ pmol/10^6 cells. This simulation suggests that equilibrium between R^s, surface receptor and free receptors in an intracellular compartment may exist and shuttling between activated cell surface receptor, R_s^* and $R^{m'}$. R^m equilibrium may enhance the recycling receptor pool.